Geological Society, London, Special Publications

Genetic diversity of manganese deposition in the terrestrial geological record

Supriya Roy

Email alerting service	click here to receive free e-mail alerts when new articles cite this article
Permission request	click here to seek permission to re-use all or part of this article
Subscribe	click here to subscribe to Geological Society, London, Special Publications or the Lyell Collection

Notes

Lyell
Collection

Genetic diversity of manganese deposition in the terrestrial geological record

SUPRIYA ROY

Department of Geological Sciences, Jadavpur University, Calcutta – 700 032, India

Abstract: Terrestrial manganese deposits formed by hydrothermal, sedimentary and supergene processes. Ancient analogues of modern oceanic hydrothermal deposits formed in spreading centre and subduction-related settings and those deposited from terrestrial hot springs are discussed. Sedimentary Mn oxide deposits formed in shallow water at the margins of stratified oceans above the redoxcline during sea-level changes. Mn carbonate deposits probably formed by diagenesis through Mn oxyhydroxide reduction coupled with organic matter oxidation. Climatic variation, and basin water stratification, responsible for Mn concentration, were manifestations of atmospheric CO_2 content prompted by tectonism. Supergene manganese enrichment in continental weathering profiles was mainly dictated by climate, topography and drainage systems.

Manganese deposits of diverse genetic types occur in the terrestrial geological record (Roy 1981). These were produced by direct hydrothermal activity, sedimentary processes, and continental weathering. Although the processes may be interrelated, each involves distinct mechanisms that place the deposits into specific genetic types. Some of these processes are best understood in preset-day depositional sites. The ancient environments were determined by the intensity and style of tectonism, volcanism and hydrothermal activity, the composition of the atmosphere and the hydrosphere, and the development of the biosphere, which all varied with time. It is my intention to unfold the total panorama of the environmental evolution during different time envelopes that produced a variety of manganese deposits in the past. Only major deposits and those providing distinctive evidence of their environment of deposition will be considered here.

Hydrothermal manganese deposits

Hydrothermal concentration of manganese as generally small deposits is fairly common in the geological record particularly during the Phanerozoic eon. These deposits are often stratabound, but may also occur as irregular bodies and epithermal veins in a large variety of host rocks. In many places, these ancient stratabound orebodies display characteristic tectonic, rock-association, mineralogical and chemical signatures that permit their correlation to deposits that are now being generated hydrothermally in the marine realm at or near spreading centres, mid-plate seamounts, and subduction-related island-arc settings. Emission of hydrothermal solution in shallow continental basins (e.g. lakes) has also produced stratabound manganese deposits (Nicholson 1990). Vein-type hydrothermal deposits are hosted mainly in volcanics of wide-ranging compositions as well as in a variety of sedimentary rocks of different ages.

A number of deposits from active plate margins such as those of the northern Apennine assemblage (Bonatti *et al.* 1976), Pindos and Othris zones (Robertson & Varnavas 1993), and the Olympic Peninsula deposit (Park 1946) demonstrate their derivation from mid-ocean ridge settings (Table 1) with the volcanic rocks showing only MORB-type chemistry. Similar settings for hydrothermal manganese deposits have been reported from the Austrian Alps, Ethiopia and Japan.

Subduction-related stratabound and vein-type hydrothermal manganese deposits have been assigned different palaeotectonic settings such as fore-arc terraces, small inter-arc basins, shallow marginal basins and trenches adjacent to continental plate margins, and back-arc basins. The deposits are mostly hosted in sedimentary rocks (radiolarian chert, volcaniclastic rocks and hemipelagic rocks) overlying island-arc type basalts, andesite, dacite, and rhyolite. Different models have been expounded to explain the occurrences of these deposits in the given settings such as upward Mn-bearing fluid expulsion (at temperatures $\leq 100°C$) by compaction and dewatering of subducting sediments in oceanic island-arcs (for discussions see Glasby 1988), and subduction of a mid-ocean ridge at a continental margin. However, determining the precise palaeotectonic setting of an ancient hydrothermal manganese deposit is a difficult task and a holistic assessment of all

Table 1. *Hydrothermal manganese deposits of mid-oceanic ridge type*

	Northern Apennine, Ophiolitic Complex, Italy	Pindos Geotectonic, Zone, Greece,	Othris, Greece,	Olympic Peninsula, USA
Age & geological sequence (bottom to top),	Late Jurassic; peridotite–gabbro–MOR basalt, radiolarian chert	Jurassic–Early Cretaceous; MOR basalt–metalliferous mudstone–radiolarian chert–red shale	Early Triassic to Cretaceous; late ultramafics–basalt/dolerite dykes–MOR basalt–chert and shale	Eocene; MOR basalt–pelagic limestone–argillite
Position of Mn and Mn–Fe–rich rocks	Mn-rich deposit at the base of Late Jurassic chert close to basalt–chert contact	Mn-rich deposit within radiolarites at the top of the sequence	Lensoid/stratified Mn deposit in chert–shale	Mn-rich lenses at the limestone–basalt contact
Mn-rich rock chemistry	Mn/Fe max. 768; low content of Ni, Co Cu, Zn; U/Th 1; total REE low; negative Ce anomaly	Mn/Fe 39 to 1086; very low Cu, Ni content	Mn/Fe 19 to 244; very low Cu, Ni, Co content	–
Other features	Fe–Cu–Zn sulphide deposits within basalt; low- to medium-grade seafloor hydrothermal metamorphism	Massive sulphide deposits in pillow basalts	Cu-rich pyrite as dykes and veins in mafic rock underlying chert-Mn horizon; Mn is either distal to hydrothermal discharge or related to off axis low temperature hydrothermal activity	Weak seafloor metamorphism
Modern analogues	TAG hydrothermal field, MAR 26° N	–	TAG area on MAR 26° N	–
References	Bonatti *et al.* (1976)	Robertson & Varnavas (1993)	Robertson & Varnavas (1993)	Park (1946)

geological and geochemical features is necessary. For example, the deposits of Manga Chrome, Smith Prospect (Sierra Nevada), Buckeye, Blue Jay, South Thomas (Franciscan Assemblage; Table 2) and that of Bald Knob, Carolina (Late Proterozoic; Flohr 1992) are geochemically similar but were formed in different tectonic environments and sometimes even by different processes. The mineral assemblages of these manganese deposits are also non-specific with respect to their palaeotectonic setting.

The chemistry of the ancient island-arc type-manganese deposits generally indicates their hydrothermal derivation (Table 2), although a dual imprint of hydrothermal and hydrogenous processes in the composition of manganese

crusts from similar present-day environments has been documented (Hein *et al.* 1988). The original geological setting of these ancient deposits is determined by the character and dominance of the volcanic and associated sedimentary rocks. Island-arc tholeiite, calc-alkaline basalt, andesite, dacite, and rhyolite are characteristic of a subduction-related setting including marginal basins and trenches and back-arc settings. The presence of volcaniclastic sediments, greywacke, biological detritus and radiolarites characterizes the subduction-related environments.

The Franciscan assemblage, California, demonstrates all attributes of a subduction-related setting. The question, however, is whether these

manganese deposits were produced in that setting or their presence there is merely incidental. Crerar *et al.* (1982) suggested that the manganese deposits at Blue Jay and South Thomas were created at a mid-ocean ridge setting similar to the present Galapagos Mounds situation and then transported to the present location. They did not, however, rule out a back-arc setting for these deposits. Huebner & Flohr (1990), on the other hand, suggested that the formation of these same deposits took place in marginal trenches of converging plate boundaries. Despite the controversy on the original site of formation of these deposits, the hydrothermal source for them and their present position in the subduction-related setting are valid. That various processes could operate in that tectonic setting is clearly shown by the Buckeye deposit. This deposit, while associated with a number of hydrothermal deposits of the Franciscan assemblage, has been shown to have formed by anoxic/suboxic diagenesis from a continental-margin sediment source rather than from hydrothermal solution (Hein & Koski 1987; Huebner & Flohr 1990; Huebner *et al.* 1992). Clearly much more work is required on such a complex assemblage before a well-integrated picture is obtained.

Much controversy exists over the original tectonic setting of the Troodos Massif, Cyprus and the Semail Nappe, Oman. Their generation was attributed to oceanic spreading centres analogous to the setting in different sectors (12° to 14°S and 21°N) of the East Pacific Rise today (Table 3; Fleet & Robertson 1980; Robertson & Boyle 1983). By contrast, smaller extensional regimes at supra-subduction zones were inferred as their locale of formation (Table 3; Pearce *et al.* 1984). Such controversies notwithstanding, manganese deposition is not affected because hydrothermal processes can operate in tectonic settings of both types. Hajash & Chandler (1981) conducted experiments reacting seawater with basalt, rhyolite and andesite at temperatures between 200 and 500°C, water/rock mass ratios between 5 and 50 and 1 kbar pressure and showed that similar ore-forming solutions were produced, a finding consistent with observations in natural situations.

Ancient hydrothermal manganese deposits also occur in continental settings as stratabound layers and veins in rocks of different varieties and ages. The stratabound San Francisco deposit, Mexico, overlies a lacustrine formation in a Tertiary continental-volcanic province. The ores (braunite, pyrolusite) interfinger with travertine and are spatially contiguous with iron deposits. Zantop (1978) concluded that a continental hot spring deposited iron and manganese in the oxygenated lacustrine basin. A thick travertine apron overlies the Pleistocene stratabound hydrothermal manganese deposit at Golconda, Nevada, while in the Burmister deposit, Arizona (Late Pliocene) travertine is interlayered with Mn oxides (Hewett *et al.* 1963, cited by Roy 1981). Similar interlayering of Mn oxide with travertine has been produced by the currently active Akan hot spring, Hokkaido, Japan (Hariya 1980).

Hydrothermal vein deposits rich in manganese minerals derived from terrestrial hot springs are common. Rarely economic, these vein deposits may or may not be genetically or temporally linked to their host rocks. Thus, many of them are hosted in igneous rocks (varying from basalt to rhyolite) which might possibly supply the ore solutions. O'Reilly (1992) inferred that the vein-type New Ross manganese deposit, Canada, occurring in granite, was formed from a hydrothermal fluid 'exsolved' during final crystallization of the host rock. Other vein deposits occur in both clastic and chemical sedimentary rocks where the hydrothermal solution, derived from an external source, circulated through fractures in the host rocks.

The veins show diverse manganese mineralogy. Low-temperature veins consist of pyrolusite, cryptomelane, psilomelane, hollandite and todorokite, whereas others, formed from relatively higher temperature solutions, exhibit braunite, bixbyite, hausmannite, huebnerite and/or Mn silicates (rhodonite, bustamite, tephroite), Mn carbonate and Mn sulphide (alabandite). Barite, fluorite, calcite and quartz are characterisic accessory minerals (for details see Roy 1981, table 38). In many cases, the Mn-rich veins show spatial and temporal relations with hydrothermal base metal sulphides and gold-silver mineralization (for summary see Roy 1981).

Sedimentary manganese deposits

Sedimentary manganese deposits easily outclass the other types in respect of size and spatial and temporal distributions. These are hosted in sequences consisting of a variety of rock types, mostly sedimentary, rarely volcanic rocks, many of which provide useful information on tectonic setting and geochemical environment. Some of these rocks share a common genetic heritage with these deposits. Sedimentary manganese deposits evolve through a sequence of stages promoting supply of the metal from a source or

Table 2. *Hydrothermal manganese deposits in subduction-related tectonic setting*

	Palaeotectonic setting	Age	Volcanic rock-type	Associated sedimentary rocks	Position of Mn-ores	Chemical composition of Mn-ores	Other features/remarks
Toqumea, Tonga island (Hein et al. 1990)	(= Tonga Ridge, fore-arc terrace)	Early Miocene	Unknown	Volcaniclastic sediments	Veins, lenses, volcaniclastic rocks	Max. Mn/Fe 2596, max. Cu 202, Co 257, Ni 63, Ba 8420 (ppm)	–
Eua, Tonga Island (Hein et al. 1990)	(= Tonga Ridge, fore-arc terrace)	Mid-Eocene–Early Oligocene	Unknown	Limestone, weathered volcaniclastic sandstone	Stratiform layer in limestone; enrichment in volcaniclastic sandstone	Mn/Fe max. 448; max. Cu 440, Co 4240, Ni 775, Ba 12500 (ppm)	–
Franciscan Assemblage		Late Jurassic–Early Cretaceous					
Blue Jay, South Thomas (Crerar et al. 1982; Huebner & Flohr 1990)	Marginal basin	Late Jurassic–Early Cretaceous	Alkaline basalt	Radiolarian chert and minor shale	As lenses interbedded with chert	Hydrothermal field in Fe-Mn-(Ni + Cu + Co × 10 diagram; very low U and Th values, pronounced negative Ce anomaly	MOR setting also possible; may be similar to the Galapagos Mound deposits

Deposit	Tectonic setting	Age	Volcanic association	Host rock	Occurrence	Geochemistry	Comments
Buckeye (Hein and Koski 1987; Huebner & Flohr 1990; Huebner et al. 1992)	Subduction-related trench at continental plate margins*	Late Jurassic–Early Cretaceous	None	Chert–shale overlying greywacke	Chert hosted	Mn/Fe 80; Cu, Co low, some enrichment in Ni, Zn; very low U and Th values	Metamorphosed to blueschist facies
Manga Chrome and Smith Prospect, Sierra Nevada, USA (Flohr & Huebner 1992)	Back-arc basin	Mid-Triassic–Early Jurassic	Island-arc tholeiite and calc-alkaline basalts (as clast)	Chert with volcanic clasts, argillites	As lenses enclosed in radiolarian chert	Plots in hydrothermal field; very low U and Th values	Metamorphosed to prehnite-actinolite facies (325°C, 2 kbar)
Florida Group Buena Vista, Solomon Island (Taylor 1976)	Island arc	Late Cretaceous–Miocene	Island arc tholeiite, andesite	Ochres, sinters, ironstone of Hanesavo Beds	Lenses of Mn oxide overlie ironstone and goethite–nontronite ochres	Mn/Fe 2.5 to 45; Cu, Co, Zn very low	Massive Cu-sulphide in mafic volcanics
Neogene Green Tuff belt, Japan (Moritani 1976; Hariya & Tatsumi 1981)	Subduction-related shallow marginal basin	Miocene	Andesite, dacite, rhyolite	Chert, argillite	Beds, lenses and veins in cherts	Unknown	Sometimes occur in outer zones of Kuroko base metal deposits (Ex. Manoka deposit)
Viti Levu, Fiji (Colley & Walsh 1987)	Small inter-arc basin	Late Oligocene–Mid-Miocene	Basalt transitional between arc-type and MORB	Hemipelagic Al-rich sediments; Fe-rich chalcedony; red clay; nontronitic clay	Within hemipelagic sediments associated with Fe-rich chalcedony and red clay	Plots in hydrothermal field in Fe–Mn–(Ni+Cu+Co) × 10 diagram	Enriched in both eruptive and erosional products of adjacent arcs

*This deposit is included here as integral part of the Franciscan hydrothermal assemblage, but the Mn-flux in the Buckeye deposits was probably derived by sub-oxic sediment diagenesis

Table 3. *Hydrothermal manganese deposits of Troodos Massif and Semail Nappe*

	Troodos Massif, Cyprus	Semail Nappe, Oman
Palaeotectonic Setting	Oceanic crust formed by sea floor spreading of mid-oceanic ridge type (Robertson & Boyle 1983; Varga & Moores 1985); supra-subduction spreading zone type (Pearce *et al.* 1984; Moores *et al.* 1984)	Oceanic crust formed by sea-floor spreading of mid-ocean ridge type (Fleet & Robertson 1980; Robertson & Boyle 1983); formed in a spreading centre in a marginal ocean in supra-subduction zone (Pearce *et al.* 1984)
Age and geological sequence (bottom to top)	Late Cretaceous to Early Tertiary Harzburgite, gabbro, sheeted dykes, lower pillow lava, upper pillow lava, pelagic chalk, radiolarite	Early Cretaceous Harzburite–gabbro–sheeted dykes–trondhjemite–high level gabbro, lower lava, upper lava, metalliferous and/or pelagic sedments, exotic melange
Volcanic rock type,	Lower pillow lavas largely basaltic andesites (also subordinate dacite and keratophyre); upper pillow lavas mostly olivine basalts (also limburgite and picrite)	Lower lavas and pillow basalts (MORB type) with gradation to underlying sheeted dykes; upper lavas are basic, intermediate to acidic having island-arc affinities
Position of Mn/Fe–Mn-rich rocks	Mn halo around Fe–Cu-sulphides at the contact of lower lava and upper lava	Fe mounds with Mn within lowermost part of upper lava; Fe–Mn umbers within upper lava and overlie pillowed and brecciated upper lava
Fe–Mn-rich rock geochemistry	Basal umber: Fe_2O_3 62.2%, MnO 2.0%, Ba 756 ppm, Cu 3 ppm, Ni 336 ppm Higher dark umber: Fe_2O_3 42.9%, MnO 18.5%, Ba 1190 ppm, Cu 1400 ppm, Ni 190 ppm Negative Ce anomaly	Fe-rich mound: Fe_2O_3 9.5%, MnO 1.2%, Ba 13 ppm, Cu 15 ppm, Ni 17 ppm Black umber mound: Fe_2O_3 15.8%, MnO 26.2%, Ba 80 ppm, Cu 1361 ppm, Ni 160 ppm Supra lava umber: Fe_2O_3 26.3%, MnO 7.3%, Ba 216 ppm, Cu 527 ppm, Ni 303 ppm Negative Ce anomaly
Other features/ indications	Fe–Cu sulphides present at the contact of lower and upper pillow lavas	Hydrothermal base metal sulphides present in lower lavas showing Mn halo
Modern analogues	EPR 12°–14°S (Robertson & Boyle 1983); FAMOUS and AMAR areas on MAR (Varga & Moores 1985)	EPR 21°N hydrothermal field (Robertson & Boyle 1983)

multiple sources, transport to a basin, and direct deposition or concentration aided by early diagenesis. Optimum efficiency at these stages in the past has been determined by the compositional evolution of the atmosphere and the hydrosphere. In contrast with modern large-scale deep-sea deposition, the geological settings of most ancient manganese deposits indicate formation in shallow-water basin-margin regimes. Direct bacterial oxidation–reduction of manganese, reported to occur in modern deposits and laboratory culture, has not been considered because its signature in ancient deposits is still ambiguous.

Evolution of the atmosphere and hydrosphere

The composition of the atmosphere and hydrosphere were initially controlled by mantle degassing followed progressively by photosynthesis and organic carbon burial. On the primitive Earth, a calculated solar luminosity lower by about 30% was compensated by high concentrations of CO_2 (produced by tectonically mediated rapid degassing) in the atmosphere, which increased the surface temperature and prevented global freezing (Kasting 1987). CH_4 and NH_3 were present perhaps only in trace

amounts in the early atmosphere as these are destroyed by photochemical reactions. The primitive atmosphere, therefore, was probably dominated by CO_2 (+CO) followed by N_2 with traces of H_2 reduced sulphur gases (Kasting 1993). Oxygen was present only in very low concentration (Cloud 1972, 1980 cited by Holland 1984; Kasting 1993). With time, photosynthetically produced oxygen and its increased relative proportion due to organic carbon burial gradually overwhelmed the volcanic flux of reduced gases. Kasting et al. (1993) speculated a more reduced state of the upper mantle in the primitive Earth and a progressive oxidation with time. They suggested that the evolution of mantle redox conditions and the state of oxidation of the atmosphere are closely interlinked.

Atmosphere and hydrosphere oxygenation exerted a primary control on deposition of sedimentary ore deposits such as those of manganese and iron. Kasting (1987) proposed

a three-stage box model which was subsequently refined to indicate progressive increase in pO_2 in the Precambrian atmosphere-ocean system (Kasting 1992, 1993). A modified version of this model is given in Table 4.

Atmosphere and hydrosphere were thus modified at different times in terms of relative CO_2 versus O_2 concentrations and temperature, which influenced the geochemically controlled exogenic processes. Tectonic activity, differing in intensity and perhaps in style, was the driving force for the modifications of atmosphere–hydrosphere composition (Berner et al. 1983; Des Marais et al. 1992). Biological activity, particularly photosynthesis, had also an important role to play, but to be optimally effective a favourable tectonic domain was necessary. Initially produced photosynthetic oxygen was largely consumed by acidic volcanic gases and Fe^{2+} sinks. Conversely, tectonically induced organic carbon burial and/ or decrease in volcanic/hydrothermal activity

Table 4. *Anoxic–oxic evolution of the atmosphere and hydrosphere during the Precambrian (modified after Kasting 1987)*

Stage	I	II	III	IV
Time envelope	c. 3.8 to between 2.4 and 2.0 Ga*	Between 2.4 and 2.0–1.9 Ga*	c. 1.9–0.9 Ga	c. 0.9–0.6 Ga
Atmosphere	Reducing; p_{O_2} c. 10^{-14} PAL max.†	Oxidizing; $p_{O_2} \approx 0.03$ PAL max.†	Oxidizing; $p_{O_2} \approx 0.002$ PAL min.†	Oxidizing
Hydrosphere (surface)	Reducing with oxygen oases: $p_{O_2} \approx 0.08$ PAL max.†	Oxidizing	Oxidizing	Oxidizing
Hydrosphere (deep)	Reducing	Reducing	Oxidizing	Intermittently oxidizing and reducing
Sediment isotopic characteristics	$\delta^{13}C \approx 0\permil$ $\delta^{34}S$ −4 to +4‰	Increased $\delta^{34}S$ values	–	$\delta^{34}S$ −10 to +20‰‡; unusually low $^{87}Sr/^{86}Sr$ in carbonates of 800–600 Ma§; strongly negative $\delta^{13}C$ between 850–670 Ma and 610–590 Ma‖, otherwise positive values

* Transition of Stages I and II at 2.4 Ga fixed based on data on detrital uraninite and pyrite and a restricted range of $\delta^{34}S$ values (Walker & Brimblecombe 1985; Lambert & Donnelly 1991). The time of transition may be shifted to c. 2.0 Ga if red beds are proved to have formed first at about 2.0 Ga.
† Kasting (1992, 1993)
‡ Lambert & Donnelly (1991)
§ Veizer et al. (1983)
‖ Knoll et al. (1986).

could gradually lead to the concentration of oxygen in the atmosphere. Orogenic events in the Late Proterozoic produced continental clastic detritus that were weathered by drawdown of atmospheric CO_2 leading to decreased temperature and initiation of glaciation. By contrast, increase in tectonic activity and volcanic/hydrothermal input of CO_2 led to greenhouse conditions and deglaciation.

During the Archaean, the atmosphere was strongly depleted in oxygen (Table 4). A very low sulphate concentration in the hydrosphere with insignificant fractionation of sulphur isotopes have been proposed (Walker & Brimblecombe 1985; Grotzinger & Kasting 1993); the $\delta^{34}S$ values for sedimentary rocks of Archaean age fall in a narrow range (Lambert & Donnelly 1991) and $\delta^{13}C$ values are close to 0‰.

A considerable increase in the concentration of seawater sulphate occurred in the Early Proterozoic (2.5–2.3 Ga) and its range of $\delta^{34}S$ values increased. Enhanced levels of photosynthesis in the Early Proterozoic, coupled with a gradual decline in production of oxygen-sinks such as Fe^{2+}, produced oxygen that could oxidize reduced sulphur species and also augment oxygen buildup of the atmosphere (Lambert & Donnelly 1991). The available $\delta^{13}C$ values in marine carbonates deposited throughout the Early and Mid-Proterozoic times stayed close to 0‰. (Schidlowski et al. 1983 cited by Lambert & Donnelly 1991). Carbonate carbon of Late Proterozoic age (c. 900–550 Ma), however, shows variable positive $\delta^{13}C$ values (indicating burial of organic carbon) interspersed with short-lived stints of negative values (800–670 Ma and 610–590 Ma; Knoll et al. 1986; Derry et al. 1992) correlated to glacial events. The higher ratios of $^{87}Sr/^{86}Sr$ in carbonates precipitated from seawater is correlated with greater continental erosion and supply, whereas this ratio is lower during times of strong hydrothermal activity. The mantle-like Nd isotope values of early Precambrian iron-formations, decreasing to much lower values with time, indicate that Nd inputs to the ocean gradually shifted from hydrothermal to continental source (Derry & Jacobsen 1990).

Stratified oceans were initiated during the prevailing high atmospheric CO_2 conditions during the Archaean with oxygenated surface water at basin margins (oxygen oases; related to shallow-water colonies of photosynthetic organisms?) and anoxic deep water (Table 4). With increase in p_{O_2} in the atmosphere by Early Proterozoic time, the entire surface waters became oxygenated while the deep-water zone remained reducing. Records of sea-level changes

(transgression–regression cycles) during that period are common (Beukes 1983; Gauthier-Lafaye & Weber 1989; Hein & Bolton 1993). Sea-level changes were caused evidently by increase in seafloor generation and enhancement of greenhouse gases in the atmosphere through tectonically induced volcanism and hydrothermal activity. Stratification of basin water was lost by further increase in atmospheric p_{O_2} by around 1.9 Ga (Table 4).

In the Late Proterozoic, however, the scenario changed again (Table 4). The break-up of the Mid-Proterozoic supercontinent (Lambert & Donnelly 1991) probably led to massive drawdown of atmosphere CO_2 (due to increased silicate weathering) and organic carbon burial (indicated by positive excursions of $\delta^{13}C$). This decreased the surface temperature to such an extent that global glacial events took place. At least four glacial events (Knoll et al. 1986) occurred during 850–590 Ma, intervened by stratified basins, transgressions and ocean anoxic events (OAE) during interglacial periods. Strong negative $\delta^{13}C$ excursions coincided with the Sturtian (850–670 Ma) and the Varangian (610–590 Ma) glacial events (Knoll et al. 1986). Seafloor hydrothermal activity is inferred to have been accentuated during the continental breakup as indicated by the unusually low $^{87}Sr/^{86}Sr$ ratio in 800–600 Ma carbonates (Veizer et al. 1983).

During the Late Proterozoic and Early Phanerozoic, the atmosphere and the entire hydrosphere were highly oxygenated approaching present p_{O_2} values. However, during that time evidence of short and fairly long-time changes in atmosphere and hydrosphere compositions have been indicated by a highly variable record of $\delta^{13}C$ values. Volcanism and other geological and biological processes, produced a greenhouse environment and rise of surface temperature many times (Fig. 1; Berner 1991). Such greenhouse-induced global warming took place at different times in the Early Palaeozoic and Mesozoic (Jenkyns 1980; Berner 1991). By contrast, cold climate prevailed during the Late Palaeozoic and the Late Cenozoic as indicated by the carbon cycle (Berner 1991), a conclusion that is in agreement with other independent estimates. During warm intervals and a positive $\delta^{13}C$ excursion, the oceans were again stratified and sea-level changes (transgression–regression cycles) attended by ocean anoxic events were operative. Transgression and upwelling were linked during regional deepening of the shelf areas (Jenkyns 1980) and organic matter was supplied from both the flooded continental area and the plankton blooms.
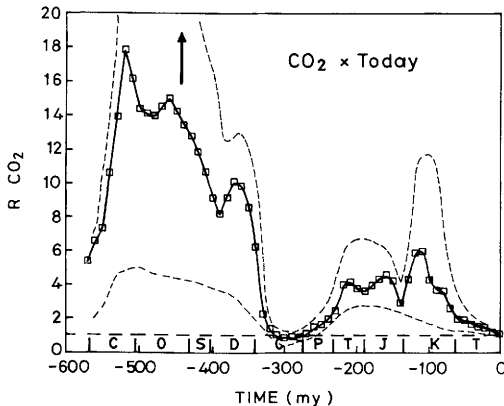
Fig. 1. Best estimate, or standard reference, curve of R_{CO_2} versus time. The arrow denotes that early Palaeozoic R_{CO_2} values may be higher. The dashed lines represent a rough estimate of error. (Berner, R. A. 1991. American Journal of Science, 291, 371. Reprinted by permission of American Journal of Science.)

Stratified basins: manganese concentration and deposition

The Black Sea, a classic example of a stratified basin, serves as a model for metal concentration in the H_2S-producing anoxic water column overlain by oxygenated water. Dissolved Mn^{2+} accumulates in the anoxic water and migrates by vertical advection–diffusion to the redox interface (Spencer & Brewer 1971); it reaches maximum concentration (c. 500 ppb) close to the interface. Above the redoxcline, Mn oxyhydroxide particulates form by oxidation of Mn^{2+} which sink back to the anoxic water and are dissolved. Similar stratified water columns develop in certain fjords (Saanich Inlet, Jacobs & Emerson 1982; Cariaco Trench, De Baar et al. 1988; Framvaren fjord, Jacobs et al. 1985) where Mn^{2+} behaves in the same manner. Only where the redoxcline impinges on the continental shelf of the Black Sea are Mn oxyhydroxides precipitated and retained (Sevast'yanov & Volkov 1966 cited in Roy 1981).

The euxinic deeper waters of the Black Sea have often been held responsible for supporting organic-rich black shale deposition. However, Calvert (1990) determined that the sediments accumulating now under anoxic conditions are poor in organic matter while Holocene sapropel (with 20 wt% organic carbon) underlying the surface sediments were deposited when the bottom waters were oxic. Therefore, the production of black shale was not dependent on water

column anoxia but rather on high organic productivity in oxygenated water (Pedersen & Calvert 1990 cited by Calvert & Pedersen 1993). Anoxic waters are not prerequisites for black shale deposition, rather black shale formation consumes oxygen from overlying waters and turns them anoxic.

Marine transgression during warm climate was causally related to stratification of the ocean when deep circulation was suppressed and oxygen solubility decreased. During transgression, the inundated continental areas supplied substantial organic debris which, together with the primary productivity in the surface water, transferred a large amount of organic matter to the bottom of the stratified epicontinental and ocean basins (Jenkyns 1980; Hallam 1987). The organic matter was bacterially degraded which further decreased oxygen content in the sediments and the bottom water and produced black shales on burial. High rates of deposition and burial of organic carbon, signalled by positive excursions of $\delta^{13}C$, have been inferred to have taken place during ocean anoxic events (OAE) causing global accumulation of black shales, for example during Early Toarcian, Late Cenomanian and Early Turonian times (Schlanger et al. 1987). Black shales are genetically related to Mn-rich carbonate deposits.

Source and transport of manganese

The precise determination of any particular source for manganese in ancient deposits is complex. Hydrothermal and terrestrial weathering processes serve as primary sources for manganese in the depositional basins, but in specific deposits the contribution of any particular source over another is difficult to assess. The few studies on REE patterns of ancient manganese deposits (Bau & Dulski 1993) indicate the source of manganese, but more such studies are needed for a clear picture. In the modern oceans it is now established that both near-field and far-field dispersal of manganese from the mid-ocean ridge hydrothermal fields takes place through buoyant plumes caught up by ocean currents (Klinkhammer & Hudson 1986). Thus, hydrothermally introduced manganese may be transported thousands of kilometres from the original site. However, the estimates made for hydrothermal component of the manganese budget in today's seawater vary widely. During the Archaean and Early Proterozoic, a more vigorous hydrothermal activity has been suggested (Holland 1984) with the associated anoxic deep-ocean as a repository of

hydrothermal manganese that was carried in solution. The magnitude of hydrothermal production of manganese probably decreased with time.

On the other hand, supply of manganese from terrestrial sources cannot be neglected. Surficial weathering processes are particularly active in humid tropical climates. Organic acids, produced by decomposing vegetation since the early Phanerozoic (Nicholson 1992), can leach manganese at different rates under various climatic conditions (Crerar et al. discussions and fig. 6a, b & c). The released manganese is carried by ground and surface waters to the lakes and the oceans. While transport of manganese to present-day northern hemisphere high-latitude lakes is fostered by acidic soil and ground water, in lower latitudes controls on river flux are more complicated.

The average concentration of dissolved manganese in river water is only a few parts per billion and its transport in ionic solution in an oxygenated environment for a long distance is difficult. Nevertheless, manganese can be transported as particulates or colloids and its gross riverine discharge to the oceans is considerable (Sapozhnikov 1970). Trefry & Presley (1982) showed that manganese transported to the ocean from coastal areas is mainly in particulate form. By contrast, Laxen et al. (1984) concluded that a major part of the $<0.015\,\mu m$ Mn size-fraction is present as Mn^{2+} species soluble in river water in addition to a significant Mn-fraction occurring as colloids. They argued that particulate and soluble Mn-fractions were decoupled under the dynamic conditions in most rivers. The Kalix river, Sweden, is discharging into the Gulf of Bothnia both dissolved and particulate manganese and the dissolved/particulate ratio varies seasonally (Pontér et al. 1992).

The coastal zone has a big role to play in the geochemical cycle of manganese during transport. Deeper water in estuaries has increased salinity and alkalinity relative to surface waters. The mixing of river water and seawater in coastal zones may lead to flocculation of dissolved manganese carried by river water which may generate coastal Mn oxide deposits (Sundby et al. 1981; Frakes & Bolton 1992). However, in the coastal environments, river discharge as well as plankton blooms can enrich the sediments in organic matter. Bacterial decomposition may consume sufficient oxygen to turn the sediments suboxic or anoxic. Manganese oxide particulates buried in such sediments are thereby reduced and the released Mn^{2+} dissolved in pore water may be recycled to enrich overlying water for export out of the coastal zone to the oceans (Sundby et al. 1981; Trefry & Presley 1982). If, however, the Mn^{2+} and dissolved bicarbonate concentration in the pore water reaches a level that exceeds the solubility product of a carbonate phase, Mn-bearing carbonates should be produced (Calvert & Pedersen 1993) and fixed within the reducing sediments thereby blocking the Mn^{2+} supply to the overlying water.

Manganese deposits:
the Archaean inauguration

No manganese ore deposits are known to have formed during the first 800 million years of Earth history. This paucity of manganese deposits reflects the deficiency of oxygen in the atmosphere and hydrosphere (Table 4). By contrast, a banded iron formation (BIF), showing very low Mn-contents, occurs in the oldest known geological sequence (Isua Supracrustals, Greenland: 3.8 Ga) and continued to form throughout the Archaean. Preferential deposition of iron may have been facilitated by its lower solubility with respect to manganese, its faster rate of oxidation by limited photosynthetically derived oxygen and/or by photochemical oxidation of Fe^{2+} by solar UV radiation in the absence of the ozone screen (Cairns-Smith 1978; Braterman et al. 1983, 1984, all cited by Anbar & Holland 1992). Experiments conducted by Anbar & Holland (1992) showed that photochemical oxidation of Mn^{2+} is also possible, but the rate is much slower than it is for Fe^{2+}; where both Mn and Fe are present in solution the rate of Mn^{2+} oxidation is decreased further.

Manganese deposits first started to form in Late Archaean time probably corresponding to the development of oxygen oases in the otherwise reducing hydrosphere (Table 4). Only a few deposits were formed during that time and these were spatially limited (Table 5). The deposits in Rio das Velhas Supergroup (Brazil) and Chitradurga Group (India) are restricted to the upper sedimentary rocks in greenstone belts. Manganese carbonate formed originally in carbon-rich pelitic sediments in geosynclinal setting of the Rio das Velhas Supergroup (Dorr et al. 1956). These deposits were metamorphosed producing Mn silicate–carbonate rocks. On the other hand, deposits of the Chitradurga group formed in the marginal shallow-water part of a basin as indicated by the associated sedimentary rocks including stromatolitic limestones (Baral 1986). The Mn oxide ores were metamorphosed to low grade.

Table 5. *Manganese deposits of Archaean age*

Age	Geological sequence	Deposits	Geological setting and features	References
c. 2.6 Ga	Chitradurga Group	Chitradurga–Tumkur, Kumsi–Hornhalli, Karnataka, India	Shallow-margin area of geosyncline; Mn oxide ore interstratified with chert & phyllite; spatially close to stromatolites	Roy (1981)
>2.6 Ga	Eastern Ghats Sequence	Kodur, Garividi, Garbham, Andhra, Pradesh, India	Shallow-water shelf (?); Mn oxide ore & Mn silicate-carbonate rocks present at different levels enclosed in calc-silicate & pelitic granulite	Roy (1981), Dasgupta *et al.* (1993)
>2.7 Ga	Rio das Velhas Supergroup	Morro do Mina, Minas Gerais, Brazil	Geosyncline; Mn silicate–carbonate rock enclosed in graphitic phyllite; mica-schist & amphibolite present	Dorr *et al.* (1956)
c. 3.0 Ga	Iron Ore Group	Joda, Kalimati, Gurda, Phagua, Mahulsukha, Orissa, India	Cratonic shelf; Mn oxide ore interstratified with shale; volcanic rocks present but not in direct contact	Roy (1981)

The Eastern Ghats sequence, India, metamorphosed to granulite facies, corresponds to Archaean high-grade terranes. Manganese oxide ores are hosted in pelitic and calc-silicate granulites (Roy 1981) while Mn silicate–carbonate rocks occur in calc-silicate granulites and garnetiferous quartzites (Dasgupta *et al.* 1993). The corresponding protoliths of the Mn oxide ores and the Mn silicate–carbonate rocks are inferred to be Mn oxide/hydroxide and Mn carbonate which had formed at different stratigraphic levels of the sequence. Signatures of the original geological setting of the Eastern Ghats sequence have almost totally been obliterated by multiple stages of deformation and metamorphism. Nevertheless, the deduced pre-metamorphic lithological sequence indicates deposition on a shallow-water shelf. The Iron Ore Group sequence, India, only incipiently metamorphosed and with orthoquartzite at the base was deposited in shallow water on a stable shelf. It neither corresponds to greenstone belts nor to high-grade terranes and is, thus, atypical of the common Archaean settings. The manganese orebodies (pyrolusite, manganite, cryptomelane, braunite) are interbedded with shale and are surficially modified by weathering.

For all these Archaean deposits, there is no evidence of *direct* volcanic/hydrothermal input of manganese. Volcanic rocks occasionally present, are separated from the orebodies by intervening rocks that show Mn content not exceeding the crustal value. Thus, it is inferred that the source of manganese was seawater. The Archaean hydrosphere was largely reducing (Table 4) permitting buildup of dissolved manganese (possibly from a hydrothermal source) which by upwelling at basin-margin oxygen oases, was oxidized and precipitated on the cratonic shelves. The formation of Mn oxides is explained without much complication, but the mode of origin of the Mn carbonates has not been deciphered (although the restriction of Mn carbonate to carbon-rich rocks in Rio das Velhas Supergroup is noteworthy), because they have been overprinted by high-grade metamorphism.

Manganese deposits: the Proterozoic development

Large-scale deposition of manganese started from the Early Proterozoic. This was possible due to oxygenation of the atmosphere and stabilization of the stratified ocean system (Stage II; Table 4). At that time dissolved Mn^{2+} was concentrated in anoxic deep water and the source was hydrothermal or terrigenous.

Middle Proterozoic (*c.* 1.9–0.9 Ga; Stage III, Table 4) sections are practically barren of manganese deposits, except for very few small occurrences developed locally. This decline in manganese deposition can be attributed to the total oxygenation of the hydrosphere that prevented the buildup of dissolved manganese. The renaissance of manganese deposition in the Late Proterozoic (Stage IV, Table 4) was a response to a number of glacial–interglacial episodes and return of stratified oceans and oxygen minimum zones.

The Kalahari manganese field, Republic of South Africa, with a potential resource of 13 600 million metric tons of ore with Mn contents between 20 and 48% is the largest among all known land-based deposits (Table 6). This deposit occurs in three different layers interstratified with BIF of the Hotazel Formation (*c.* 2.24 Ga; Stage II, Table 4) of the Late Archaean to Early Proterozoic Transvaal Supergroup (*c.* 2.64–1.9 Ga; Beukes *et al.* 1993). The cyclic Mn ore layers are mainly composed of braunite–kutnohorite assemblage (Mamatwantype; Beukes 1983; Kleyenstüber 1984). Signatures of trace and rare earth elements indicate that manganese was supplied by deep anoxic waters of a stratified ocean with a small

hydrothermal component (Beukes 1989). The $\delta^{13}C$ values of carbonates (kutnohorite, Mncalcite) in the ores range between -12 and $-16‰$ indicating that part of the carbon is derived from organic carbon oxidation (Beukes 1993). The sedimentary manganese ores of Mamatwan-type (braunie–kutnohorite), in the western extension, have been modified by later hydrothermal alteration to an assemblage of braunite II, bixbyite, hausmannite, and a host of hydrous and anhydrous Mn silicates (Wesselstype; Kleyenstüber 1984).

In the Koegas Subgroup (Ghap Group, Transvaal Supergroup), Mn oxide orebodies (psilomelane, pyrolusite, jacobsite, hausmannite, hematite) are interbedded with the Rooinekke iron formation. This iron formation, and by extension the manganese ore beds, were deposited following a major transgression (Beukes 1993). Anoxic deep seawater could be a plausible source of the metals in these deposits.

The geological setting of the Birimian Supergroup greenstone belt in the West African craton (Ghana, Ivory Coast, Burkina Faso, Mali, Eastern Liberia, Guinea) is unique among the Early Proterozoic sequences hosting manganese deposits (Table 6). More or less evenly spaced parallel belts of isoclinally folded volcanic rocks (mainly

Table 6. *Manganese deposits of Early Proterozoic age*

Age	Geological sequence	Deposits	Geological setting and features	References
c. 2.0 Ga	Sausar Group	Mansar, Chikla, Tirodi, India	Cratonic shelf; limestone–shale–orthoquartzite; no volcanic rock; Mn oxide ore beds in shale (Mansar Fm) and limestone (Lohangi Fm) metamorphosed to greenschist and amphibolite facies	Roy (1966, 1981)
c. 2.1 Ga	Francevillian Series	Okouma and Bangombé Plateaus, Gabon	Cratonic shelf; Mn carbonate interbedded with black shale, dolomite and sandstone; no volcanic rock	Gaunthier–Lafaye & Weber (1989); Hein & Bolton (1993)
c. 2.3 to 2.0 Ga	Birimian Supergroup	Nsuta, Ghana; Mokta, Ivory Coast; Tambao, Burkina Faso	Greenstone belt formed in intracontinental rift; Mn carbonate in black shale in transition zone between volcanic & sedimentary rocks	Dorr (1968); Leube *et al.* (1990)
c. 2.64 to 1.9 Ga	Hotazel Fm (*c.* 2.24 Ga) Postmasburg Group, Transvaal Supergroup	Mamatwan, Wessels, South Arica	Cratonic shelf; Mn oxide & Mn carbonate ore interbedded with BIF	Beukes (1983); Kleyenstüber (1984)

basalts with MORB chemistry: age *c*. 2.3–2.2 Ga; Taylor *et al.* 1992) are closely related in space with sedimentary units (chemical sedimentary rocks, volcaniclastic rocks, argillites, turbidity-current-related wackstones) that show overlapping (*c*. 2.3–2.0 Ga) ages (Leube *et al.* 1990; Taylor *et al.* 1992). An intracontinental rift setting has been suggested for this greenstone belt (Leube *et al.* 1990). A chemical sedimentary facies composed of chert and Ca–Fe–Mg carbonate is associated with black shale (δ^{13}C–18.3 to –26.7‰; Leube *et al.* 1990) that hosts rhodochrosite beds (Dorr 1968). This lithofacies occurs in transitional zones between the volcanic belts and the sedimentary units. Birimian Supergroup rocks underwent only low-grade metamorphism. Economic manganese deposits occur as supergene enrichment products in weathered zones. The ultimate source of manganese is difficult to decipher. It may only be guessed that hydrothermal activity during intracontinental rifting could supply manganese that, through recycling, was deposited as sediments.

The Early Proterozoic Moanda deposit in the Francevillian Series (*c*. 2.1 Ga; Bros *et al.* 1992), Gabon, is the largest known black-shale-hosted Mn carbonate deposit (Table 6). Rhodochrosite beds are interstratified with black shale, dolomite, and sandstone in a sequence (FBI unit) that is underlain by sandstone-conglomerate (FA unit) of the epicontinental Francevillian Series (Weber 1973 cited by Leclerc & Weber 1980; Gauthier-Lafaye & Weber 1989). The FA unit consists of fluvial clastic rocks that are overlain by a deltaic and marine sequence. The black shales in the FB 1 unit, formed during marine transgression (Gauthier-Lafaye & Weber 1989), contain an average 7% (locally >20%) total organic carbon (Hein & Bolton 1993). The δ^{13}C values of the organic matter ranges between –25 and –38‰. (Gauthier-Lafaye & Weber 1989) while for rhodochrosite δ^{13}C is –16‰ (Hein & Bolton 1993). The Mn carbonate-rich horizons consist of Mn-rich dolomite, Ca-rhodochrosite, and minor but persistent pyrite. Hein & Bolton (1993) concluded that pyrite and rhodochrosite were formed by sulphate reduction coupled with organic matter oxidation during early diagenesis. From the REE characteristics of the ore samples they also concluded that the primary manganese mineralization took place from a reducing seawater source in an epicontinental basin during a transgression–regression cycle. Hein & Bolton (1993) aptly correlated this deposit with the first stage of large-scale burial of organic carbon and rapid increase in atmospheric oxygen (Stage II; Table 4). The economic ore zone consisting of

Mn oxide was produced by oxidation of Mn carbonates during weathering.

The Proterozoic (*c*. 2.0 Ga) Sausar Group, India, including the manganese deposits (Table 6), have been complexly deformed and metamorphosed to grades ranging from low greenschist facies to upper amphibolite facies. This sequence consists of metamorphosed equivalents of a limestone–shale–orthoquartzite assemblage (Roy 1966, 1981) indicating a shelf environment. The presence of dolomite at the top (Bichua Fm) indicates further shallowing of the basin. Interbanded Mn oxide orebodies (braunite, bixbyite, hollandite, jacobsite, hausmannite) and Mn silicate–oxide rocks are interstratified with metapelites and orthoquartzites (Mansar Fm) and less commonly occur as conformable lenses in carbonate rocks of the older Lohangi Fm (Roy 1966, 1981). The protoliths of these Mn-rich rocks were Mn oxide/hydroxide sediments admixed with variable amounts of Fe, Si, and Al (Roy 1966, 1981; Dasgupta *et al.* 1990 and references therein). The Mn silicate–carbonate rocks, derived from Mn carbonate progenitor with admixed impurities, also occur as isolated pockets in the Mn oxide ore horizon of the Mansar Fm. The Mn oxide deposits are inferred to have formed on the continental shelf during a sea-level highstand, when detrital supply was minimal. Deposition above the redox interface produced Mn oxides even on the carbonate substrate (Lohangi Fm). Mn carbonate sediments in the Mansar Fm were diagenetically derived from Mn oxides by reaction with calcareous partings in isolated pools where an evaporative condition developed.

Sedimentary manganese deposits (cryptomelane, minor braunite), associated with BIF, occur in four stratigraphic horizons in the glaciogenic Late Proterozoic Santa Cruz Formation of the Jacadigo Group (900–600 Ma; Walde 1981 cited by Urban *et al.* 1992) at Urucum, Brazil (Table 7). Urban *et al.* (1992) suggested deposition of the orebodies in a narrow fjord-like basin. During glaciation, the underlying stagnant seawater was cut off from oxygen supply and was rendered anoxic by organic matter decomposition. Manganese and iron were thus mobilized from particulates and clastic grains to be concentrated in the dissolved state (compare situations in modern seasonally ice-covered lakes; Pontér *et al.* 1992 and references therein). Lateral transport of Mn^{2+} and Fe^{2+} ions to ice-free parts of the fjord or gradual regression of ice-cap promoted oxygenation and precipitation, first of iron and then of manganese dictated by their rates of oxidation and solubility difference. Climate-controlled

repeated transgression–regression of the ice-cap explains the rhythmic intercalation of the manganese ore horizons and the BIF as well as the coarse clastic zones between them. The source of the metals was seawater fed by continental run off.

The Late Proterozoic Damara Sequence, Namibia (Table 7) consists mainly of shelf facies sedimentary rocks, diamictites, and volcanic–sedimentary successions (Breitkopf 1988). The glaciogenic sequence of the Chuos Formation (750–650 Ma; Miller 1983a in Breitkopf 1988) of the Damara Sequence at Otjosondu consists of (bottom to top) lower quartzite, lower Mn horizon, BIF, upper Mn horizon, and upper quartzite (Bühn et al. 1992). These rocks have been metamorphosed to upper amphibolite facies. Protoliths identified for the Mn-rich rocks are almost pure and massive Mn–Fe oxides, interlayered Mn oxides and terrigenous sedimentary rocks and Mn–Fe enriched mudstones. Bühn et al. (1992) concluded that the Chuos Formation represents a transgressive–regressive sequence and they related transgression both to the opening of the proto-South Atlantic and the Khomas Sea and interglacial sea-level change. They inferred that the lower and the upper manganese ore horizons formed in transgressive and regressive stages respectively. The interglacial transgression facilitated the formation of almost pure Mn–Fe oxides as the supply of terrigenous detritus was interrupted. Bühn et al. (1992) invoked a hydrothermal source for manganese derived from basin-centred volcanism as an alternative to the continental supply; they considered that transport of dissolved manganese in the Late Proterozoic oxidizing environment was not possible. But manganese is still supplied to the oceans by rivers in the present-day oxidizing environment. Moreover, Bau & Dulski (1993) determined a positive Ce anomaly from these ores and concluded their derivation from a continental source.

Late Proterozoic glaciation was most widespread in China. Three episodes are recorded of which the second, Nantuo ice age (c. 720–680 Ma; Fan et al. 1992), was most prominent. In the Datangpo black shale sequence, correlated with an interglacial interval of the Nantuo ice age, several Mn carbonate beds, interstratified with black shale, occur at Xiangtan, Minle, Datangpo, Guchen, Tangganshan, and other areas (Fan et al. 1992; Table 7). In most deposits, tillites have been recognized at the base and top of the black shale sequence. No iron formation has been recorded. Fan et al.

Table 7. *Manganese deposits of Late Proterozoic age*

Age	Geological sequence	Deposits	Geological setting and features	References
900–600 Ma	Santa Cruz Fm, Jacadigo Group	Urucum, Brazil	Glaciogenic sequence; four Mn oxide beds mostly intercalated with BIF; glaciomarine dropstones common in the sequence	Urban et al. (1992)
c. 750–650 Ma	Chuos Fm, Damara Sequence	Otjosondu, Namibia	Interglacial transgressive–regressive sequence; BIF sandwiched between Mn oxide horizons; metamorphosed to upper amphibolite facies	Bühn et al. (1992)
c. 720–680 Ma	Datangpo Sequence, Nantuo ice age	Xiangtan, Minle, Datangpo, Tangganshan, China	Interglacial transgressive sequence; Mn carbonate hosted in black shale underlain and overlain by tillite; no BIF	Fan et al. (1992)
c. 800 Ma	Penganga Group	Tamsi, Guda, Kanpa, India	Transgressive sequence; no evidence of glaciation; Mn oxide ore interbedded with chert enclosed in limestone; no BIF in the sequence	Chaudhuri et al. (1989); Roy et al. (1990)

(1992) inferred that the Mn carbonate deposits were formed in shallow estuarine basins during interglacial transgression aided by biochemical (algal) mediation.

Manganese deposits occur in the Late Proterozoic sedimentary sequence of the Penganga Group (Table 7), developed in Godavari Valley, a major continental rift area in India. Chaudhuri et al. (1989) first assigned a Group status to the Penganga sequence and established the following stratigraphy (bottom to top): basal arkosic sandstone on granitic basement, shale–sandstone intercalation, limestone, glauconitic sandstone, and shale. Volcanic rocks are absent and the sequence was not metamorphosed. The finely laminated thick limestone sequence has been inferred to have developed during a transgressive phase. The Mn oxide ores, interstraified with chert, are enclosed in the limestone section. Ores partly retained the primary minerals (todorokite and birnessite) that were in places converted to manganite, braunite, and bixbyite during late diagenesis (Roy et al. 1990). This partial conversion clearly shows that both braunite and bixbyite with extremely low iron-contents can form during late diagenesis. The ores have been assigned a sedimentary origin with a seawater source. In spite of a Late Proterozoic age, the Penganga sequence does not show any evidence of glaciation.

Manganese deposits: the Phanerozoic finale

During the Phanerozoic, biodiversity increased and CO_2 content of the atmosphere fluctuated considerably (Fig. 1). This variation of CO_2 content was caused by changes in rates of sedimentary burial of organic matter, weathering of silicates and carbonate rocks on the continents and the release of CO_2 by volcanic and metamorphic processes (Berner 1991). Short and long-term interludes of warm climate corresponded with higher inputs of greenhouse gases to the atmosphere. Consequently, the oceans became intermittently stratified in conjunction with changes in sea level.

The development of sedimentary manganese deposits during the Phanerozoic has been more or less temporally coeval with stratified oceans, events of transgression and ocean anoxia (Cannon & Force 1983; Frakes & Bolton 1984, 1992; Force & Cannon 1988). During periods of greenhouse warming, dissolved manganese was concentrated in the deep anoxic part of the stratified basins. Cannon & Force (1983) and Force & Cannon (1988) visualized precipitation of Mn oxide/hydroxide at the feather edge of

transgressive wedges on the continental shelf whereas Frakes & Bolton (1984) modelled manganese deposition mainly during marine regression at the Groote Eylandt deposit, Australia (Fig. 2). The veil effect (flocculent fallout from river water) in the coastal areas by change in salinity and the shoreward bottom transport of manganese particulates by tidal lag (broom effect) have been considered as important parameters for generation of Mn oxide deposits (Fig. 2). Manganese carbonate deposition has also been correlated with transgression and ocean anoxic events, in dysaerobic and anoxic environments (Force & Cannon 1988; Jenkyns et al. 1991).

The Middle Ordovician Taojiang deposit, China, is the only well-documented economic concentration of manganese of early Palaeozoic age. Manganese carbonate ore beds occur in a sequence of black shale, Fe–Mn-bearing limestone, and calcareous claystone (Table 8). The ore-bearing horizon marks the transitional stage between peak transgression and the initiation of regression (Fan et al. 1992). The Mn carbonate ore (rhodochrosite, kutnohorite, Mn-calcite) shows a wide range of negative $\delta^{13}C$ values (−5.8 to −17.8‰, Okita & Shanks 1992; −9 to −22‰, Fan et al. 1992). Okita & Shanks (1992) concluded that particulate MnO_2 was originally precipitated and coupled oxidation of organic matter and reduction of MnO_2 produced diagenetic Mn carbonates with negative $\delta^{13}C$ values.

During the early Toarcian ocean anoxic event in Europe, Mn carbonate beds, in association with black shale, formed in rifted basins in continental margins in Austria, Germany, Hungary, Italy and Switzerland (Jenkyns et al. 1991). These widely scattered Mn carbonate beds are coeval (tenuicostatum to early falciferum Zones) and were formed just prior to black shale deposition. The deposits are also similar in character. The best-studied and economically viable deposit at Úrkút, Hungary is representative of these stratiform Mn carbonate occurrences.

The Mn carbonate deposits at Úrkút, Hungary, occurs in a marine sequence composed of bioclastic limestone, radioclarian clay marlstone and black shale (Table 8). The monomineralic rhodochrosite ore beds occur at two stratigraphic intervals within radiolarian clay marlstone just below black shales. Polgári et al. (1991) contended that euxinic conditions existed when sedimentation of marlstone took place. The ore beds lack pyrite, and show paucity of flora and fauna. The $\delta^{13}C$ values for rhodochrosite (average −14.5‰) show a negative linear correlation with Mn-content and a negative
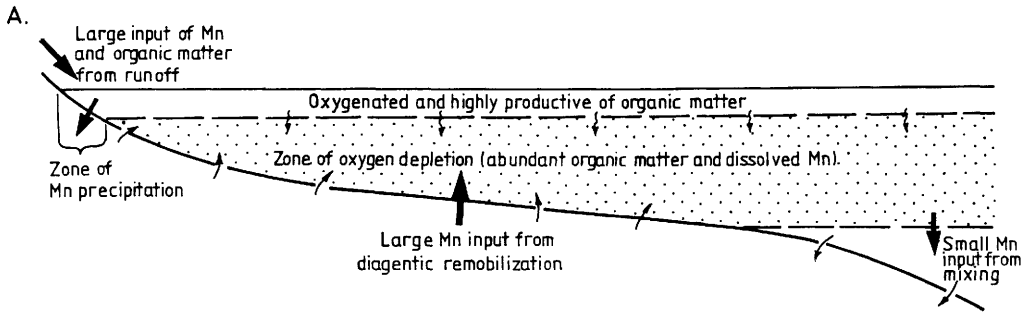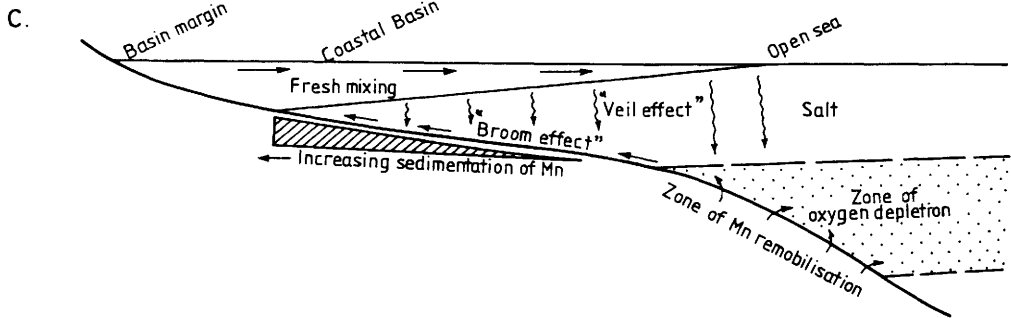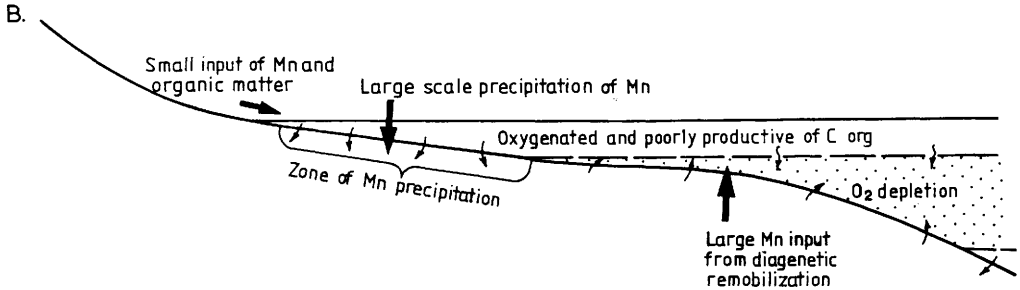
Fig. 2. (a) Relationships during marine transgression, showing narrow zone of Mn accumulation and concentration of dissolved Mn in water column. (b) Relationship during marine regression with abundant diagenetic remobilization and wide zone of final Mn precipitation. (c) Manganese sedimentation in coastal zone of intracratonic basin, showing veil effect (flocculant fallout) from saline mixing and broom effect (bottom transport and concentration) from tidal activity. (Reproduced from Frakes & Bolton 1984).

expotential correlation with total organic carbon (TOC) indicting that rhodochrosite formed by early diagenesis involving organic matter oxidation. Polgári et al. (1991) concluded that dissolved manganese of unknown source accumulated in anoxic seawater and precursor Mn oxyhydroxides formed on the continental shelf above the redoxcline. Reduction of this Mn oxyhydroxide was coupled with organic matter oxidation producing Mn carbonates. Additionally, Mn reduction and coupled oxidation of FeS (originally produced by seawater sulphate

reduction) might have taken place, inhibiting pyrite formation (cf. Aller & Rude 1988).

The giant stratiform rhodochrosite deposit at Molango, Hidalgo State, Mexico, is the only major manganese deposit in North America. The ore horizon occurs in the Chipoco facies (Table 8) at the base of the Taman Fm (marine limestone and shale; Kimmeridgian), and is in contact with the underlying Santiago Fm (calcareous and pyrite-rich black shale; Late Callovian to Late Oxfordian). A shallowing water depth from the lower Santiago Fm

Table 8. *Manganese deposits of Phanerozoic age*

Age	Geological sequence	Deposits	Geological setting and features	References
Early Oligocene	Early Kharkovian	Nikopol, Ukraine	Shallow-marine sandstone–glauconitic claystone; facies change from Mn oxide to Mn carbonate ore	Varentsov & Rakhmanov (1980)
	Early Kharkovian	Chiatura, Georgia	Same as above	Bolton & Frakes (1985)
Late Cretaceous	–	Imini-Tasdremt, Morocco	Mn oxide beds interstratified with dolomite sandwiched between non marine sequences	Force *et al.* (1986)
Middle Cretaceous	Mullaman beds	Groote Eylandt, Australia	Mn oxide ores overlying glauconitic calcareous siltstone with Mn carboante and pyrite resting on Precambrian sandstone	Frakes & Bolton (1984)
Late Jurassic	Taman Fm, Chipoco facies	Molango, Mexico	Rhodochrosite beds in marine limestone–shale sequence overlying black shale of Santiago Fm	Okita (1992)
Early Jurassic	–	Úrkút, Hungary	Rhodochrosite beds in radiolarian clay marlstone underlying black shale	Polgári *et al.* (1991)
Middle Ordovician	Modaoxi Fm	Taojiang, China	Mn carbonate beds occur in a sequence of black shale, limestone and calcareous shale	Fan *et al.* (1992)

to the Chipoco facies is indicated and Okita (1992) suggested that the manganese deposits formed 'either at the culmination of regression or the onset of transgression'. In the basal part of the Chipoco facies ('A-Bed'), pyritiferous Mn carbonate occurs which is overlain by the high-grade ore zone consisting of fine laminations of rhodochrosite alternating with silty shale. In the lower half of this ore zone, pyrite is rare, but magnetite and maghemite are present in silty layers. The ore zone peters out in the middle Chipoco interval. The lowermost part of the Chipoco facies is devoid of marine fauna, indicating dysaerobic to anaerobic conditions during sedimentation; the older Santiago Fm was deposited in an euxinic environment (Okita 1992).

Several features such as very low pyrite content, presence of Fe oxides, presence of rhodochrosite as the exclusive Mn phase, and the upsection evolution from dysaerobic to more oxidizing conditions provide the keys to the formation of the Mn carbonate ore zone. Aller & Rude (1988) predicted that Mn oxide (taken as MnO_2) could be an important agent for oxidizing both sulphur and organic carbon. The rhodochrosite from the Molango deposit shows negative $\delta^{13}C$ values (average $-13‰$) and an antithetic correlation between $\delta^{13}C$ values and Mn content (Okita *et al.* 1988 cited by Okita 1992). Therefore, manganese reduction corresponded to organic matter oxidation and rhodochrosite and the Fe oxides were early diagenetic products. Cannon & Force (1983) suggested a stratified ocean model for the Molango deposit. However, Okita (1992) favoured river transport of manganese to the depositional basin considering the restricted spatial and temporal nature of the deposit against its enormous Mn metal reserve.

At Groote Eylandt, Australia, a large shallow-water stratiform manganese deposit occurs in the intra-cratonic Carpentaria basin. The orebody occurs in the Mullaman Beds (Late Albian to

Early Cenomanian) that uncomfortably overlies Middle Proterozoic sandstone (Table 8; Frakes & Bolton 1984). The deposit, composed mainly of Mn oxide pisoliths and ooliths, extends for about 22 km with a maximum thickness of 9 m (average 3 m). Immediately below this ore zone, a pyritiferous and glauconite-bearing calcareous siltstone is present, which also contains rhodochrosite and Mn calcite. The most interesting and critical feature recognized in the ore zone is the presence of both normal- and inverse-graded units of Mn oxide pisoliths and ooliths. Frakes & Bolton (1984) interpreted that the pisoliths and ooliths are of primary accretionary origin developed in a shallow-water marine environment. They also inferred that manganese, from a terrestrial source, was concentrated in the dissolved state in transgression-induced oxygen-deficient basin water during the Late Albian. The normal-graded ore units were possibly formed during peak transgression and the inverse-graded units were developed during marine regression (Fig. 2).

The Cenomanian–Turonian sedimentary Mn oxide deposits of Imini–Tasdremt belt, Morocco, are hosted in dolomite (Table 8). Stratiform orebodies are restricted to three levels in the dolomite horizon, two near the base and the third near the top. Pyrolusite, hollandite, coronadite and janggunite constitute the ore. Force et al. (1986) observed that the ore-bearing dolomite horizon has been totally modified by diagenesis. In the Imini area a fossiliferous carbonate unit occurs. A marine, probably an inner shelf, depositional environment is indicated by the faunal assemblage. A rapid marine transgression recorded in this marginal sequence was largely responsible for supplying dissolved manganese from anoxic part of a stratified ocean to the Imini-Tasdremt area (Force et al. 1986; Thein 1990). A mixing zone of saline and fresh water is thought to have played a key role in the diagenetic modification of host carbonates (dolomitization) as well as the manganese deposits (oxidation of Mn carbonates). Alternatively, primary precipitation of manganese may have taken place in shifting mixing zones where anoxic seawater mixed with ground water delivered dissolved manganese to zones of fresh oxygenated ground water where precipitation of oxides occurred (Force et al. 1986). Following this mixing-zone model, Thein (1990) inferred that the anoxic zone of the stratified basin was supplied with manganese from continental weathering and that mixing occurred during sea-level highstand.

Very large deposits of unmetamorphosed Mn oxide and carbonate ores of Early Oligocene age occur at Chiatura (Georgia), and Nikopol and Bol'shoi Tokmak (Ukraine) in shallow-marine intracratonic setting. The ore-bearing sequence at Chiatura uncomfortably overlies either the crystalline basement or Late Cretaceous limestone resting on the basement (Table 8). The ore-bearing Oligocene sequence at Nikopol and Bol'shoi Tokmak overlies basement rocks of the Ukrainian shield (Table 8). Features common to these deposits include, (a) a large number of ore-beds and lenses interstratified with or enclosed in orthoquartzite and glauconitic claystone, (b) nodular (oolitic and pisolitic) structure of the ores, and (c) a basinward facies change from oxides to carbonates. Such a zonal arrangement of manganese oxide, oxide plus carbonate, and carbonate at the Chiatura deposit was attributed to Eh variation from shallow to deep water during deposition (Betekhtin 1937 cited by Roy 1981). On the basis of aerobic faunal record in the manganese carbonate zone, this interpretation was rejected and later diagenetic change of Mn oxide to Mn carbonate was suggested (Strakhov & Shterenberg 1966; Strakhov et al. 1970; Danilov 1974 all cited by Roy 1981). Sapozhnikov (1970) proposed that dissolved Mn-rich anoxic water from this basin, on upwelling, supplied manganese to a near-shore environment to be deposited through oxidation in shallow-water.

Bolton & Frakes (1985) suggested that the Chiatura deposit formed during a transgressive–regressive cycle in a restricted arm of the Paratethys. They established that the Mn oxide and Mn carbonate ooliths and pisoliths formed by accretion in a shallow-marine low-energy setting, in contradiction to a diagenetic origin proposed by earlier workers. Bolton & Frakes (1985) identified both normal- and inverse-graded bedding in Mn oxide ooliths and pisoliths. They proposed that during transgression, manganese supplied by terrestrial weathering was concentrated in the dissolved state in oxygen-depleted seawater. The Mn carbonates formed in deeper offshore areas where reducing conditions prevailed while in shallow near-shore oxygenated regions Mn oxides were deposited. Following the Groote Eylandt model, Bolton & Frakes (1985) proposed that normally graded units were deposited in a late transgressive period and the inverse grading was formed by a combination of basin shallowing, increasing energy levels and greater oxygenation during the regressive phase.

Hein & Bolton (1992) presented carbon and oxygen isotope data from the Mn carbonate ores of Nikopol. $\delta^{13}C$ values vary between $-9‰$ and $-16.5‰$. PDB (mean $-11.9‰$) and $\delta^{18}O_{SMOW}$

values show a range of +26.7‰ to +30.8‰ (mean +29.6‰). These data indicate that carbon was almost equally derived from seawater bicarbonate and organic carbon degradation at a relatively low temperature. Hein & Bolton (1992) inferred that Mn oxyhydroxide probably formed initially and Mn carbonates were early diagenetically derived through the coupled reaction of organic matter oxidation and Mn reduction.

In summary, all important Phanerozoic manganese deposits were formed during transgression–regression cycles triggered by greenhouse conditions followed by oxygenation. However, all such cycles did not necessarily produce manganese deposits as, for example, during the early Palaeozoic. Most manganese deposition took place in intracratonic and rifted continental-margin basins and the source of manganese was inferred to be terrestrial weathering rather than oceanic hydrothermal effluent. Coastal processes have exerted important controls on the geochemical cycle of manganese (veil and broom effect) and these in concert with sea-level changes formed concentrated manganese deposits. Manganese carbonate deposits probably always formed during early diagenesis. Carbon isotope studies on Mn carbonates from the deposits at Taojiang, Urkút, Molango and Nikopol showed that Mn oxyhydroxide was initially precipitated and was reduced coupled with organic matter oxidation leading to formation of Mn carbonate. Conversely, the manganese oxide deposits of Imini–Tasdremt area were probably produced by conversion of originally formed Mn carbonate to oxide in a ground water–seawater mixing zone. The apparent lack of temporal as opposed to spatial contiguity of most important sedimentary manganese deposits through geological history has been rightly pointed out by Frakes & Bolton (1992) as enigmatic and only a satisfactory resolution of this issue will indicate how many genetic models need to be evoked to explain the origin of these deposits.

Supergene manganese deposits in the weathered zone

Concentrations of manganese in zones of terrestrial weathering are common and can yield commercial deposits. Climate and the initial Mn content in the source rock are crucial determinants in this process of manganese ore formation. For example, in arid to semi-arid conditions only thin and sporadic layers of Mn oxides (desert varnish) are formed by local surficial migration and no commercial deposit is recorded. In temperate and subarctic climatic zones in higher latitudes of the northern hemisphere, humate-rich podzolic soil permits high mobility for manganese released by acidity and high-rate organic decay during weathering. As a result, manganese is neither retained as residual concentration nor allowed to reprecipitate within the weathered zone; it is entirely exported to the sedimentary cycle in lakes and bogs. Humid tropical climate with abundant rainfall and vegetation, in concert with suitable topography (e.g. plateaus), drainage system, and parent rock composition, can produce a manganese deposit within the zone of weathering (Crerar et al. 1972, fig. 6a, b, & c). The role of organic acids (humic acid, fluvic acid; formed by decay of vegetation) in chemical weathering of rocks and the release of manganese dissolved in acidic ground water has been emphasized by Crerar et al. (1972) and Nicholson (1992).

The leaching of manganese and iron may take place together or one in preference to the other. Selective leaching of manganese with respect to iron can occur by enzymatic microbial reduction. In the Al–Fe–Mn triad, the solubility of manganese is maximum (as is its mobility) and hence, during downward movement of iron and manganese in solution, a change in Eh–pH may lead to precipitation of iron in preference to manganese and an effective separation between the two may take place. Where the weathered profile attains sufficient thickness, the upper zone is depleted in manganese which travels deeper and is reprecipitated in the lower zone (Roy 1981 and references cited therein). Pracejus et al. (1988) invoked electrochemical reactions between Fe^{2+} (dissolved in ground water or adsorbed on kaolinite) and Mn^{4+} in the zone of weathering at Groote Eylandt deposit, Australia. According to their model, by these reactions Mn^{4+} in the oxide minerals was reduced and dissolved with consequent deposition of Fe^{3+} phases (goethite, hematite) and clay minerals. On transportation, dissolved Mn^{2+} cemented pisolitic and oolitic primary sedimentary ore, or formed mangcrete (Pracejus et al. 1988).

The sedimentary Mn oxide ore deposits of the Iron Ore Group (Bihar and Orissa) and the Dharwar Supergroup (Karnataka and Goa), India, show considerable chemical reworking in the weathered zone (Roy 1981). In many deposits, aluminium and iron (laterite) are characteristically concentrated in the upper zone and manganese in the lower zone of the weathered profile. In the Sausar Group, a large supergene deposit extending for about 1.5 km and of a thickness exceeding 130 m occurs at Dongri Buzurg. The

deposit was formed by oxidation of pre-existing metamorphosed Mn oxide (with Mn^{2+} and Mn^{3+}) and Mn silicate rocks (Roy 1981).

The rocks most amenable to supergene concentration of manganese in the weathering zone are Mn-rich carbonates followed closely by Mn silicate–carbonates. Mn oxides are either formed in situ by oxidation of the carbonates or through dissolution, limited vertical and lateral migration, and reprecipitation. Most sedimentary Mn carbonate deposits discussed in the earlier section, particularly those located in humid tropical climates, yielded supergene cappings of Mn oxide/hydroxide ores that often form large deposits. The best known deposits of this type occur in Brazil (Serra do Navio, Amapa; Morro da Mina, Minas Gerais; Azul, Para), Gabon (Moanda), Ghana, Ivory Coast, Burkina Faso, Eastern Liberia, and Mexico (Molango); smaller deposits occur at Urkút, Hungary, Philipsburg and Butte, USA, and Janggun mine, South Korea (for detailed discussion see Roy 1981). The ages of weathering in these deposits are poorly known, but it is suggested that supergene enrichment took place chiefly during the Cenozoic.

The only evidence of Proterozoic weathering producing commercial Mn oxide ores at the cost of manganiferous carbonates comes from deposits formed in palaeo-sinkholes in dolomites of the Campbellrand Subgroup (Ghap Group; Transvaal Supergroup) in South Africa. Development of these sinkholes and supergene enrichment of manganiferous dolomites to Mn oxides are attributed to weathering that took place preceding the deposition of the overlying Proterozoic Gamagara Formation of the Olifantshoek Group (Grobbelaar & Beukes 1986). Such Mn oxide deposits are well-developed in Bishop, Glosam, and Lohatlha mine areas and are composed dominantly of bixbyite and braunite, which might have formed by diagenesis (cf. Roy et al. 1990) of supergene Mn^{4+}-rich oxides after burial and superimposition of the Gamagara Formation. A later weathering cycle, probably during the Cenozoic, produced psilomelane and pyrolusite (Grobbelaar & Beukes 1986).

References

ALLER, R. C. & RUDE, P. D. 1988. Complete oxidation of solid phase sulfides by manganese and bacteria in anoxic marine sediments. *Geochimica et Cosmochimica Acta*, **52**, 751–765.

ANBAR, A. D. & HOLLAND, H. D. 1992. The photochemistry of manganese and the origin of banded iron formation. *Geochimica et Cosmochimica Acta*, **56**, 2595–2603.

BARAL, M. C. 1986. Archean stromatolite from Dodguni belt of Karnataka craton, India. *Journal of the Geological Society of India*, **25**, 328–333.

BAU, M. & DULSKI, P. 1993. Distribution of rare-earth elements in Precambrian sedimentary Fe-, Mn-, and P-deposits. *16th International Colloquium of Africa Geology, Extended Abstracts*, 27–28.

BERNER, R. A. 1991. A model for atmospheric CO_2 over Phanerozoic time. *American Journal of Science*, **291**, 339–376.

——, LASAGA, A. C. & GARRELS, R. M. 1983. The carbonate-silicate geochemical cycle and its effect on atmospheric carbon dioxide over the past 100 million years. *American Journal of Science*, **283**, 641–683.

BEUKES, N. J. 1983. Palaeoenvironmental setting of iron-formation in the depositional basin of the Transvaal Supergroup, South Africa. *In*: TRENDALL, A. F. & MORRIS, R. C. (eds) *Iron-formation: Facts and Problems*. Elsevier, Amsterdam, 139–209.

——1989. Sedimentological and geochemical relationships between carbonate, iron-formation and manganese deposits in the early Proterozoic Transvaal Supergroup, Griqualand West, South Africa. *28th International Geological Congress, Washington DC, Abstracts*, **1**, 143.

——1993. A review of manganese deposits associated with the early Proterozoic Transvaal Supergroup in Northern Cape Province, South Africa. *16th International Coloquium of Africa Geology, Extended Abstracts*, 37–38.

——, GUTZMER, J. & KLEYENSTÜBER, A. S. E. 1993. *Excursion Guide to Iron and Manganese Deposits of the Transvaal Supergroup, Griqualand West*. IGCP Project 318, South Africa Field Workshop, September 1993.

BOLTON, B. R. & FRAKES, L. A. 1985. Geology and genesis of manganese oolites, Chiatura, Georgia, U.S.S.R. *Geological Society of America Bulletin*, **96**, 1398–1406.

BONATTI, E., ZERBI, M., KAY, R. & RYDELL, H. S. 1976. Metalliferous deposits from the Apennine ophiolites: Mesozoic equivalents of modern deposits from oceanic spreading centre. *Geological Society of America Bulletin*, **87**, 83–94.

BREITKOPF, J. H. 1988. Iron formation related to mafic volcanism and ensialic rifting in the southern margin zone of the Damara orogen, Namibia. *Precambrian Research*, **38**, 111–130.

BROS, R., STILLE, P., GAUTHIER-LAFAYE, F. & WEBER, F. 1992. Sm–Nd isotopic dating of Proterozoic clay material: an example from the Francevillian sedimentary series, Gabon. *Earth and Planetary Science Letters*, **113**, 207–218.

BÜHN, B., STANISTREET, I. G. & OKRUSCH, M. 1992. Late Proterozoic outer shelf manganese and iron deposits at Otjosondu (Namibia) related to the Damaran oceanic opening. *Economic Geology*, **87**, 1393–1411.

CALVERT, S. E 1990. Geochemistry and origin of the Holocene sapropel in the Black Sea. *In*: ITTEKKOT, V., KEMPE, S., MICHAELS, W & SPITZY, A. (eds) *Facts of Modern Biogeochemistry.* Springer, Berlin, 326–352.

—— & PEDERSEN, T. F. 1993. Geochemistry of Recent oxic and anoxic marine sediments: implications for the geological record. *Marine Geology*, **113**, 67–88.

CANNON, W. F. & FORCE, E. R. 1983. Potential for high-grade shallow-marine manganese deposits in North America. *In:* SHANKS, W. C. III, (ed.) *Cameron Volume on Unconventional Mineral Deposits.*, Society of Mining Engineers, American Institute of Mining, Metallurgical and Petroleum Engineers, New York, 175–189.

CHAUDHURI, A. K., DASGUPTA, S., BANDOPADHYAY, G., SARKAR, S., BANDOPADHYAY, P. C. & GOPALAN, K. 1989. Stratigraphy of the Penganga Group around Adilabad, Andhra Pradesh. *Journal of the Geological Society of India*, **34**, 291–302.

COLLEY, H. & WALSH, J. N. 1987. Genesis of Fe-Mn deposits of southwest Viti Levu, Fiji. *Transactions Institution of Mining and Metallurgy, Section B, Applied Earth Sciences*, **96**, 201–212.

CRERAR, D. A., CORMICK, R. K. & BARNES, H. L. 1972. Organic controls on the sedimentary geochemistry of manganese, *Acta Mineralogica-Petrographica*, **20**, 217–226.

——, NAMSON, J., CHYI, M. S., WILLIAMS, L. & FEIGENSON, M. D. 1982. Manganiferous cherts of the Franciscan assemblage: I. General geology, ancient and modern analogues, and implications for hydrothermal convection at oceanic spreading centers. *Economic Geology*, **77**, 519–540.

DASGUPTA, S., BANERJEE, H., Fukuoka, M., BHATTA-CHARYA, P. K. & ROY, S. 1990. Petrogenesis of metamorphosed manganese deposits and the nature of the precursor sediments. *Ore Geology Reviews*, **5**, 359–384.

——, HARIYA, Y. & MIURA, H. 1993. Compositional limits of manganese carbonates and silicates in granulite facies metamorphosed deposits of Garbham, Eastern Ghats, India. *Resource Geology Special Issue*, **17**, 43–49.

DE BARR, H. J. W., GERMAN, C. R., ELDERFIELD, H. & VAN GAANS, P. 1988. Rare earth element distribution in anoxic waters of the Cariaco Trench. *Geochimica et Cosmochimica Acta*, **52**, 1203–1219.

DERRY, L. A. & JACOBSEN, S. B. 1990. The chemical evolution of Precambrian seawater: evidence from REES in banded iron formations. *Geochimica et Cosmochimica Acta*, **54**, 2965–2977.

——, KAUFMAN, A. J. & JACOBSEN, S. B. 1992. Sedimentary cycling and environmental change in the Late Proterozoic: evidence from stable and radiogenic isotopes. *Geochimica et Cosmochimica Acta*, **56**, 1317–1329.

DES MARAIS, D. J., STRAUSS, H., SUMMONS, R. E & HAYES, J. M. 1992. Carbon isotope evidence for the stepwise oxidation of the Proterozoic environment. *Nature*, **359**, 605–609.

DORR, J. V. N. 1968. Primary manganese ores. *Proceedings, 23rd Congress, Sociedade Brasiliera do Geologia*, 1–12.

——, COELHO, I. S. & HOREN, A. 1956. The manganese deposits of Minas Gerais, Brazil. *22nd International Geological Congress, Symposium on Manganese*, **3**, 279–346.

FAN, D., LIU, T. & YE, J. 1992. The process of formation of manganese carbonate deposits hosted in black shale series. *Economic Geology*, **87**, 1419–1429.

FLEET, A. J. & ROBERTSON, A. H. F. 1980. Ocean-ridge metalliferous and pelagic sediments of the Semail Nappe, Oman. *Journal of the Geological Society, London*, **137**, 403–422.

FLOHR, M. J. K. 1992. Geochemistry and origin of the Bald Knob manganese deposit, North Carolina. *Economic Geology*, **87**, 2023–2040.

—— & HUEBNER, J. S. 1992. Mineralogy and geochemistry of two metamorphosed sedimentary manganese deposits, Sierra Nevada, California. *Lithos*, **28**, 57–85.

FORCE, E. R. & CANNON, W. F. 1988. Depositional model for shallow-marine manganese deposits around black shale basins. *Economic Geology*, **83**, 93–117.

——, BACK, W., SPIKER, E. C. & KNAUTH, L. P. 1986. A ground-water mixing model for the origin of the Imini manganese deposit (Cretaceous) of Morocco. *Economic Geology*, **81**, 65–79.

FRAKES, L. A. & BOLTON, B. R. 1984. Origin of manganese giants: sea level change and anoxic-oxic history. *Geology*, **12**, 83–86.

—— & —— 1992. Effects of ocean chemistry, sea level and climate on the formation of primary sedimentary manganese ore deposits. *Economic Geology*, **87**, 1207–1217.

GAUTHIER-LAFAYE, F. & WEBER, F. 1989. The Francevillian (Lower Proterozoic) uranium ore deposits of Gabon. *Economic Geology*, **84**, 2267–2285.

GLASBY, G. P. 1988. Hydrothermal manganese deposits in island arcs and related to subduction processes: a possible model for genesis. *Ore Geology Reviews*, **4**, 145–153.

GROBBELAAR, W. S. & BEUKES, N. J. 1986. The Bishop and Glosam manganese mines and the Beeshoek Iron ore mine of the Postamasburg area. *In:* ANHAEUSSER, C. R. & MASKES, S. (eds) *Mineral Deposits of Southern Africa.* Geological Society of South Africa, Johannesburg, 957–961.

GROTZINGER, J. P. & KASTING, J. F. 1993. New constraints on Precambrian Ocean composition. *Journal of Geology*, **101**, 235–243.

HAJASH, A. & CHANDLER, G. W. 1981. An experimental investigation of high-temperature interactions between seawater and rhyolite, andesite, basalt and peridotite. *Contributions to Mineralogy and Petrology*, **78**, 240–254.

HALLAM, A. 1987. Mesozoic marine organic-rich shales. *In*: BROOKS, J. & FLEET, A. J. (eds) *Marine Petroleum Source Rocks*. Geological Society, London, Special Publications, **26**, 251–261.

HARIYA, Y. 1980. On the geochemistry and formation of manganese dioxide deposits. *In*: VARENTSOV, I. M. & GRASSELLY, G. (eds) *Geology and Geochemistry of Manganese*, **1**, E. Schweizerbart'sche Verlagsbuchhandlung, Stuttgart, 353–365.

—— & TATSUMI, M. 1981. Hydrogen isotopic composition of MnO(OH) minerals from manganese oxide and massive sulfide (Kuroko) deposits of Japan. *Contributions to Mineralogy and Petrology*, **77**, 256–261.

HEIN, J. R. & BOLTON, B. R. 1992. Stable isotope composition of Nikopol and Chiatura manganese ores, U.S.S.R.: implications for genesis of large sedimentary manganese deposits. *29th International Geological Congress*, Kyoto, Abstracts, **1**, 209.

—— & —— 1993. Composition and origin of the Moanda manganese deposit, Gabon. *16th International Colloquium on Africa Geology*, Extended Abstracts, 1150–1152.

—— & KOSKI, R. A. 1987. Bacterially mediated diagenetic origin for chert-hosted manganese deposits in the Franciscan Complex, California Coast Range. *Geology*, **15**, 722–726.

——, GEIN, L. M. & MORRISON, S. 1988. Submarine ferromanganese mineralization in active volcanic arc systems. *Pacific Congress on Marine Science & Technology, PACON 88, Proceedings*, Honolulu, Hawaii, 83–88.

——, SCHULZ, M. S. & KING, J. K. 1990. Insular and submarine ferromanganese mineralization of the Tonga-Lau Region. *Marine Mining*, **9**, 305–354.

HOLLAND, H. D. 1984. *The Chemical Evolution of the Atmosphere and Oceans*. Princeton University Press, Princeton, NJ.

HUEBNER, J. S. & FLOHR, M. J. K. 1990. *Micro-banded Manganese Formations: Protoliths in the Franciscan Complex, California*. US Geological Survey Professional Paper **1502**.

——, —— & GROSSMAN, J. N. 1992. Chemical fluxes and origin of a manganese carbonate-oxide-silicate deposit in bedded chert. *Chemical Geology*, **100**, 93–118.

JACOBS, L. & EMERSON, S. 1982. Trace metal solubility in an anoxic fjord. *Earth and Planetary Science Letters*, **60**, 237–252.

——, —— & SKEI, J. 1985. Partitioning and transport of metals across the O_2/H_2S interface in a permanently anoxic basin: Framvaren Fjord, Norway. *Geochimica et Cosmochimica Acta*, **49**, 1433–1444.

JENKYNS, H. C. 1980. Cretaceous anoxic events: from continents to oceans. *Journal of the Geological Society, London*, **137**, 171–188.

——, GECZY, B. & MARSHALL, J. D. 1991. Jurassic manganese carbonates of central Europe and the early Toarcian anoxic event. *Journal of Geology*, **99**, 137–149.

KASTING, J. F. 1987. Theoretical constraints on oxygen and carbon dioxide concentrations in the Precambrian atmosphere. *Precambrian Research*, **34**, pp. 205–29.

——1992. Models relating to Proterozoic atmosphere and ocean chemistry. *In*: SCHOPF, J. W. & KLEIN, C. (eds) *The Proterozoic Biosphere*. Cambridge University Press, New York, 1185–1187.

——1993. Earth's early atmosphere. *Science*, **259**, 920–926.

——, EGGLER, D. W. & RAEBURN, S. P. 1993. Mantle redox evolution and the oxidation state of the Archean atmosphere. *Journal of Geology*, **101**, 245–257.

KLEYENSTÜBER, A. S. E. 1984. The mineralogy of the manganese-bearing Hotazel Formation of the Proterozoic Transvaal sequence in Griqualand West, South Africa. *Transactions Geological Society of South Africa*, **87**, 257–272.

KLINKHAMMER, G. P. & HUDSON, A. 1986. Dispersal patterns for hydrothermal plumes in the South Pacific using manganese as a tracer. *Earth and Planetary Science Letters*, **79**, 241–249.

KNOLL, A. H., HAYES, J. M., KAUFMAN, A. J., SWETT, K. & LAMBERT, I. B. 1986. Secular variation in carbon isotope ratios from upper Proterozoic successions of Svalbard and East Greenland. *Nature*, **321**, 832–838.

LAMBERT, I. B. & DONNELLY, T. H. 1991. Atmospheric oxygen levels in the Precambrian: a review of isotopic and geological evidence. *Paleogeography, Paleoclimatology, Paleoecology (Global Planetary Change Section)*, **97**, 83–91.

LAXEN, D. P. H., DAVISON, W. & WOOF, C. 1984. Manganese chemistry in rivers and streams. *Geochimica et Cosmochimica Acta*, **48**, 2107–2111.

LECLERC, J. & WEBER, F. 1980. Geology and genesis of the Moanda manganese deposits, Republic of Gabon. *In*: VARENTSOV, I. M. & GRASSELLY, G. (eds) *Geology and Geochemistry of Manganese*, **2**. E. Schweizerbart'sche Verlagsbuchhandlung, Stuttgart, 89–109.

LEUBE, A., HIRDES, W., MAUER, R. & KESSE, G. O. 1990. The early Proterozoic Birimian Supergroup of Ghana and some aspects of its associated gold mineralization. *Precambrian Research*, **46**, 139–165.

MOORES, E. M., ROBINSON, P. T., MALPAS, J. & XENOPHONOTOS, C. 1984. Model for the origin of the Troodos Massif, Cyprus, and other mideast ophiolites. *Geology*, **12**, 500–503.

MORITANI, T. 1976. Tertiary manganese mineralisation in Japan. *In*: GLASBY, G. P. & KATZ, H. R. (eds) *CCOP/SOPAC Technical Bulletin*, **2**, 80–82.

NICHOLSON, K. 1990. Stratiform manganese mineralisation near Inverness, Scotland: A Devonian sublacustrine hot-spring deposit? *Mineralium Deposita*, **25**, 126–131.

——1992. Genetic types of mangane oxide deposits in Scotland: Indicators of paleo-ocean spreading rate and a Devonian geochemical mobility boundary. *Economic Geology*, **87**, 1301–1309.

OKITA, P. M. 1992. Manganese carbonate mineralization in the Molango District, Mexico. *Economic Geology*, **87**, 1345–1366.

—— & SHANKS III, W. C. 1992. Origin of stratiform sediment-hosted manganese carbonate ore deposits: examples from Molango, Mexico and Taojiang, China. *Chemical Geology*, **99**, 139–164.

O'REILLY, G. A. 1992. Petrographic and geochemical evidence for a hypogene origin of granite-hosted, vein-type Mn mineralization at the New Ross Mn deposits, Lunenburg County, Nova Scotia, Canada. *Economic Geology*, **87**, 1275–1300.

PARK, C. F. 1946. The spilite and manganese problems of the Olympic Peninsula, Washington. *American Journal of Science*, **244**, 305–323.

PEARCE, J. A., LIPPARD, S. J. & ROBERTS, S. 1984. Characteristics and tectonic significance of supra-subduction zone ophiolites. *In*: KOKELAAR, B. P. & HOWELLS, M. F. (eds) *Marginal Basin Geology*. Geological Society, London, Special Publications, **16**, 77–94.

POLGÁRI, M., OKITA, P. M. & HEIN, J. R. 1991. Stable isotope evidence for the origin of the Urkút manganese ore deposit, Hungary. *Journal of Sedimentary Petrology*, **61**, 384–393.

PONTÉR, C., INGRI, J. & BOSTRÖM, K. 1992. Geochemistry of manganese in the Kalix river, northern Sweden. *Geochimica et Cosmochimica Acta*, **56**, 1485–1494.

PRACEJUS, B., BOLTON, B. R. & FRAKES, L. A. 1988. Nature and development of supergene manganese deposits, Groote Eylandt, Northern Territory, Australia, *Ore Geology Reviews*, **4**, 71–98.

ROBERTSON, A. H. F. & BOYLE, J. F. 1983. Tectonic setting and origin of metalliferous sediments in the Mesozoic Tethys Ocean. *In*: RONA, P. A., BOSTRÖM, K., LAUBIER, L. & SMITH, K. L. JR, (eds) *Hydrothermal Processes of Seafloor Spreading Centres*. Plenum, New York, 595–663.

—— & VARNAVAS, S. P. 1993. The origin of hydrothermal metalliferous sediments associated with the early Mesozoic Othris and Pindos ophiolites, mainland Greece. *Sedimentary Geology*, **83**, 87–113.

ROY, S. 1966. *Syngenetic Manganese Formations of India*. Jadavpur University Press, Calcutta.

——1981. *Manganese Deposits*. Academic Press, London.

——, BANDOPADHYAY, P. C., PERSEIL, E. A. & FUKUOKA, M. 1990. Late diagenetic changes in manganese ores of the upper Proterozoic Penganga Group, India. *Ore Geology Reviews*, **5**, 341–357.

SAPOZHNIKOV, D. G. 1970. Geological conditions for the formation of manganese deposits of the Soviet Union. *In*: SAPOZHNIKOV, D. G. (ed.) *Manganese Deposits of Soviet Union*, Israel Program for Scientific Translations, 9–33.

SCHLANGER, S. O., ARTHUR, M. A., JENKYNS, H. C. & SCHOLLE, P. A. 1987. The Cenomanian-Turonian oceanic anoxic event. I. Stratigraphy and distribution of organic carbon-rich beds and the marine $\delta^{13}C$ excursion. *In*: BROOKS, J. & FLEET, A. J. (eds) *Marine Petroleum Source Rocks*. Geological Society London, Special Publications, **26**, 373–402.

SPENCER, D. W. & BREWER, P. G. 1971. Vertical advection-diffusions and redox potentials as controls on the distribution of manganese and other trace metals dissolved in the waters of the Black Sea. *Journal of Geophysical Research*, **76**, 5877–5892.

SUNDBY, B., SILVERBERG, N. & CHESSELET, R. 1981. Pathways of manganese in an open estuarine system. *Geochimica et Cosmochimica Acta*, **45**, 293–307.

TAYLOR, G. R. 1976. Styles of mineralisation in the Solomon islands – a review. *In*: GLASBY, G. P. & KATZ, H. R. (eds) *CCOP/SOPAC Technical Bulletin*, **2**, 83–91.

TAYLOR, P. N., MOORBATH, S., LEUBE, A. & HIRDES, W. 1992. Early Precambrian crustal evolution in the Birimian of Ghana: constraints from geochronology and isotope geochemistry. *Precambrian Research*, **56**, 97–111.

THEIN, J. 1990. Paleogeography and geochemistry of the "Cenomano-Turonian" formations in the manganese district of Imini (Morocco) and their relation to ore deposition. *Ore Geology Reviews*, **5**, 257–291.

TREFRY, J. H. & PRESLEY, B. J. 1982. Manganese fluxes from Mississippi delta sediments. *Geochimica et Cosmochimica Acta*, **46**, 1715–1726.

URBAN, H., STRIBRNY, B. & LIPPOLT, H. J. 1992. Iron and manganese deposits of the Urucum district, Mato Grosso do sul, Brazil, *Economic Geology*, **87**, 1375–1392.

VARENTSOV, I. M. & RAKHMANOV, V. P. 1980. Manganese deposits of the USSR (A Review). *In*: VARENTSOV, I. M. & GRASSELLY, G. (eds) *Geology and Geochemistry of Manganese*, **2**. E. Schweizerbart'sche Verlagsbuchhandluing, Stuttgart, 320–391.

VARGA, R. J. & MOORES, E. M. 1985. Spreading structures of the Troodos ophiolite, Cyprus. *Geology*, **13**, 846–850.

VEIZER, J., COMPSTON, W., CLAUER, N. & SCHIDLOWSKI, M. 1983. $^{87}Sr/^{86}Sr$ in late Proterozoic carbonates: evidence for a "mantle event" at 900 Ma ago. *Geochimica et Cosmochimica Acta*, **47**, 295–302.

WALKER, J. C. G & BRIMBLECOMBE, P. 1985. Iron and sulfur in pre-biologic ocean. *Precambrian Research*, **28**, 205–222.

ZANTOP, H. 1978. Geologic setting and genesis of iron oxides and manganese oxides in the San Francisco manganese deposit, Jalisco, Mexico. *Economic Geology*, **73**, 1137–1149.